Korean J. Chem. Eng., 33(3), 1095-1103 (2016)
DOI: 10.1007/s11814-015-0227-3

pISSN: 0256-1115
eISSN: 1975-7220

Multiwalled carbon nanotubes and fluoroelastomer antistatic nanocomposite for automotive fuel system components

Young Seok Lee*, Seong Hwan Park*, Jong Cheol Lee, and Kiryong Ha*,†**

*Department of Chemical Engineering, Keimyung University, Daegu 42601, Korea
**Jin-Yang Oil Seal Co., Ltd., 100-52, Galsan-dong, Dalseo-gu, Daegu 704-900, Korea
(*Received 16 June 2015 • accepted 28 October 2015*)

Abstract−Fluoroelastomer (FKM) composites, reinforced with multiwalled carbon nanotubes (MWNTs), were prepared by conventional method to determine the possibility of using MWNTs to develop an antistatic composite in automotive fuel systems. The results obtained from the composite containing 0-9 phr of MWNTs were compared. A 5 points increase in hardness was achieved with the addition of only 1 phr of MWNTs and 9 phr added FKM composite was increased 6.4 MPa in tensile strength compared to the MWNTs unfilled FKM composite. In addition, electrical conductivity increased from 0 to 1.039 Scm^{-1} with increase in the MWNTs concentration, and the dynamic damping property was increased in the rubbery state region accordingly. These phenomena can be explained by the MWNTs networks formed in FKM matrix. This research will therefore be useful in the development of an antistatic rubber composite for fuel system components, which are deformed or vibrated while in operation.

Keywords: Carbon Nanotube, Antistatic Nanocomposite, Fluoroelastomer, Mechanical Property, Electrical Property

INTRODUCTION

Fluoroelastomer (FKM) has been extensively used in seals and gaskets for automotive fuel systems because of its superior thermal resistance and excellent fuel resistance. In addition, the fluorine atoms on its backbone can provide good flame resistance and usually self-extinguishing upon removal of flame source [1-3]. However, fuel system components are required to dissipate electricity because flowing fuel can build up static charges, which may result in severe casualties [4]. Nonetheless, elastomers are generally low in electrical conductivity ($<10^{-13}$ Scm^{-1}) and do not meet the requirements for many applications by themselves [5,6]. To improve mechanical and electrical properties of elastomers, carbon black has been readily used as the filler material in the rubber industry to prepare composites with greatly improved strength, stiffness, and wear resistance, etc. [7,8]. The electrical conductivity also can be improved significantly up to 10^{-4} Scm^{-1} by additional incorporation of carbon black at higher filler loading [5]. However, high loading of fillers can create problems related to processing, curing, and in the performance of product such as reduction of sealing ability due to increase of compression set. Recently, in an attempt to decrease the loading of particulate filler in the elastomeric matrix and to create new material systems with superior properties, various nanomaterials such as layered silicates, carbon or clay fibers, and carbon nanotubes (CNTs) have been extensively used as reinforcing fillers in an elastomeric matrix. Among these, CNTs are considered to be the most promising candidate to produce composites with good mechanical properties, excellent electrical conductivity, thermal stability, and flame retardancy [9-12].

Since the discovery by Iijima, CNTs have received increasing attention due to their high aspect ratio and unique arrangement of carbon hexagons in tube-like fullerenes [13,14]. CNTs have exceptional mechanical properties because the two-dimensional arrangement of the carbon atoms in a graphene sheet allows the formation of strong out-of-plane bonds and makes the graphene sheet exceptionally resistant to any in-plane distortion or fracture [15]. Young's modulus of nanotube bundles, when considered as a uniform material, exceeds 1 TPa. This is particularly beneficial in the case of high-strength composites based on nanotubes [16]. In addition, CNTs have outstanding electrical properties. Other researchers have documented room temperature conductivity values of up to 10^4 Scm^{-1} for a so-called metallic CNT. There are estimations that the overall fraction of metallic CNT is around one-third of the whole material. In the case of multiwalled carbon nanotubes (MWNTs), which consist of several rolled up graphene shells, conductivity of 2×10^6 Sm^{-1} has been reported previously [15,17].

A great deal of attention is being given to MWNTs because of the possibility of improving stiffness, strength, and electrical conductivity of polymeric composites at relatively low concentrations [18-22]. For this reason, a number of studies have investigated the mechanical and electrical behavior of MWNT reinforced composites. Lan et al. [23] studied mechanical properties of MWNTs reinforced hydrogenated carboxylated nitrile-butadiene rubber, and Lorenz et al. [5] observed electrical conductivity of rubber composite based on CNT-hybrid filler systems. Their results showed that the tensile strength and electrical conductivity were remarkably improved with relatively low concentrations of MWNTs.

Our aim was to develop a new generation of rubber composites for application in automotive fuel systems that satisfy the mechanical requirements while eliminating some potential problems, such as

†To whom correspondence should be addressed.
E-mail: ryongi@kmu.ac.kr

breakage of the conductive path under stress and strain, while maintaining a low loading level of MWNTs. To this end, the influence of the MWNTs loading level on the mechanical and electrical properties of the composite has been studied. These properties were characterized by universal testing machine (UTM) and low-resistivity meter analysis. The vulcanization reaction was analyzed by using an oscillating disk rheometer (ODR), and the damping property was measured by performing dynamic mechanical analysis (DMA). In addition, the formation of MWNTs networks in FKM matrix was observed by using field emission scanning electron microscopy (FE-SEM), and the thermal stability of the composites was evaluated by thermogravimetric analysis (TGA).

EXPERIMENTAL

1. Materials

The CNTs used in this experiment were MWNTs (trade name Nanocyl® 7000), which were produced via catalytic carbon vapor deposition (CVD). Their average diameter and length are 9.5 nm and 1.5 μm, respectively, and their surface area is 205-300 m^2/g [24]. FE-SEM image of the MWNTs without further purification is shown in Fig. 1, which demonstrates the high entanglement of MWNTs. The FKM used in this study was Viton 361C (copolymer of hexafluoropropylene and vinylidene fluoride, polymer fluorine content: 66%), which is a bisphenol curative-containing pre-compound produced by DuPont. Wollastonite with trade name NYAD 400 was obtained from NYCO, and other ingredients were purchased from local companies.

2. Preparation of Composites

Two-stage mixing was performed with a 3 *l* kneader and open two-roll mixer to prepare the MWNTs/FKM composites. The first stage mixing (master batch) involved compounding the FKM, MWNTs, NYAD 400, and process aids with the kneader. The fill factor was fixed at 0.8, and the starting operation temperature of the kneader was set to 60 °C. The rotor speed was set to 30 RPM. During the second stage mixing, MgO and $Ca(OH)_2$ were added into the master batch composite as acid acceptors. Acid acceptors are necessary in FKM composites because they neutralize any hydrogen fluoride generated either during curing or upon extended ageing at high temperatures. The friction ratio of the open two-roll mixer was 1.1 : 1 and the nip gap was set to 1 mm. The mixing time was kept uniform for all composites. The names of the MWNTs/FKM composites are designated by NT 0-NT 9, with the MWNTs loading designated in parts per hundred of rubber by weight (phr) in the FKM matrix. The mixing formulations are summarized in Table 1.

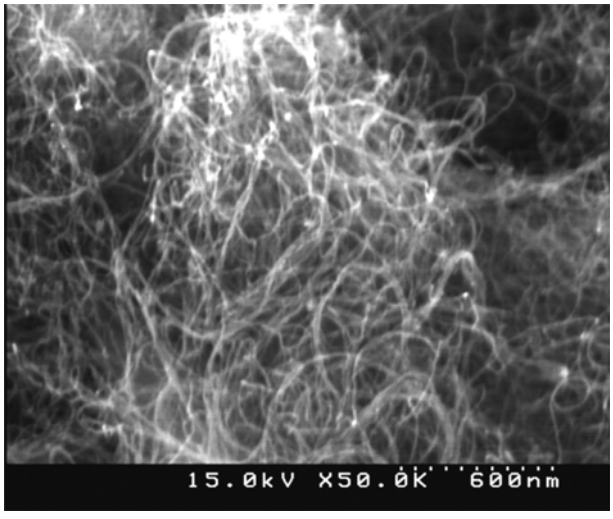

Fig. 1. SEM image of Nanocyl® 7000.

Table 1. Formulations of the MWNTs/FKM composites

Ingredients	Content (phr)[a]
Polymer (FKM)[b]	100
Wollastonite[c]	30
MWNTs[d]	0-9
Carnauba-wax	2
$Ca(OH)_2$	4
MgO	7

[a]Parts per hundred parts of rubber
[b]Viton 361C
[c]NAYD 400
[d]Nanocyl® 7000

3. Characterization Techniques

The curing behavior of the MWNTs/FKM composites was measured at the processing temperature of 170 °C using ODR (KHR-2000, Kunhaw engineering, Korea). Vulcanizate sheets with a thickness of 2 mm were prepared by curing the composites in a hot press (80 ton) at 170 °C, and they were cut using ASTM Die C. The tensile strength and elongation at break were measured following ASTM D 412 method with dumbbell shaped specimens using UTM (Kunhaw engineering, Korea). In addition, specimens that had been thermally aged in a circulating air oven at 180 °C for 70 h were tested to investigate heat resistance of the composite. The mechanical properties were measured for three specimens in each case, and the average values were calculated and reported. The compression set and hardness were measured in accordance with ASTM D 395 method B and D 2240, respectively. The dynamic mechanical properties of the MWNTs/FKM composites were measured by dynamic mechanical analysis (DMA Q800, TA instruments Co., USA) under tension mode. The specimens were prepared as a rectangular specimen. Temperature sweep experiments were carried out in the range of −50 to 120 °C with a heating rate of 3 °C/min at a constant frequency of 10 Hz and strain rate of 0.05%. The electric conductivity was measured for both the original and extended specimen from 10% to 50% using Loresta GP resistivity meter (MCP-T610, Mitsubishi Chemical Co., Japan) connected with an ESP-type four-pin probe. The probe inter-pin distance was 5 mm and the pin diameter was 2 mm. The rectangular specimen (size: 70 mm×10 mm×2 mm) was clamped between the jaws of a manual stretching machine, and three measurements were conducted on each specimen surface under room temperature. The applied voltage used for measuring the electrical conductivity was 10 V, and the measurement point was always located at the center of the sheet. Electrical conductivity is calculated by using Eqs. (1) and (2):

$$\rho_v = R \times RCF \times t \quad (1)$$

$$\sigma = 1/\rho_v \quad (2)$$

where ρ_v [Ω·cm] is volume resistivity, R [Ω] is resistivity, RCF is resistivity correction factor, t [cm] is thickness of sample, and σ [Scm^{-1}] is electrical conductivity. The RCF value is equipment-dependent and was given as 4.532, according to value settings from the manufacturer. The average of three values in each case was taken to be the electrical conductivity of the MWNTs/FKM composites. The thermal stability of the composite due to MWNTs content level was carried out using TGA (SDT Q600, U.S.A) from room temperature to 800 °C at a heating rate of 10 °C/min under N_2 flow. To observe the morphology of the composite, specimens were prepared by two methods. One method was cryo-fracture of the composite using liquid nitrogen, and the other was thermal treatment at 500 °C for 3 min in air to eliminate the FKM polymer, followed by sputtering gold on the resulting surface. FE-SEM (S-4300, Hitachi, Japan) was used to observe the morphology and dispersion of the MWNTs in the composite.

RESULTS AND DISCUSSION

1. Vulcanization Characteristics

The vulcanization characteristics were evaluated by calculating {maximum torque (M_H) - minimum torque (M_L)}, scorch time (ts_1), cure time (tc_{90}), and tc_{90} - ts_1 reflecting the chemical cross-linking density, scorch time, optimum cure time, and curing reaction rate of the composites [6,25], respectively. These properties were measured at 170 °C, and their values are listed in Table 2. The M_H increased up to 4 phr MWNTs loading, after which it remained constant. Meanwhile, M_L increased linearly from 0.83 to 3.10 N·m with increasing the MWNTs concentration in the FKM matrix. It was observed that the difference between the maximum and minimum torque values of each composite decreased after 4 phr. The ts_1 began to increase after 5 phr loading, while tc_{90} increased linearly from 0 phr (390 s) to 9 phr (639 s) with increasing MWNTs loading. This result demonstrates that the curing reaction rate decreases as the MWNTs concentration in the FKM matrix increases. It is postulated that the presence of inorganic MWNT in the matrix is obstructing the curing reaction of the FKM by affecting the mobility of the polymer chains, where other scientists have also observed similar behavior in various composite systems [26,27].

Table 2. Vulcanization characteristics of the MWNTs/FKM composites at 170 °C

Composites	M_H-M_L (N·m)	Ts_1 (s)	Tc_{90} (s)	Tc_{90}-ts_1 (s)
NT0	2.99	150	390	240
NT1	3.10	151	410	259
NT2	3.18	147	443	296
NT3	3.21	154	481	327
NT4	3.19	149	512	363
NT5	3.10	148	548	400
NT6	2.97	150	588	438
NT7	2.66	162	617	455
NT8	2.32	163	640	477
NT9	2.14	174	639	465

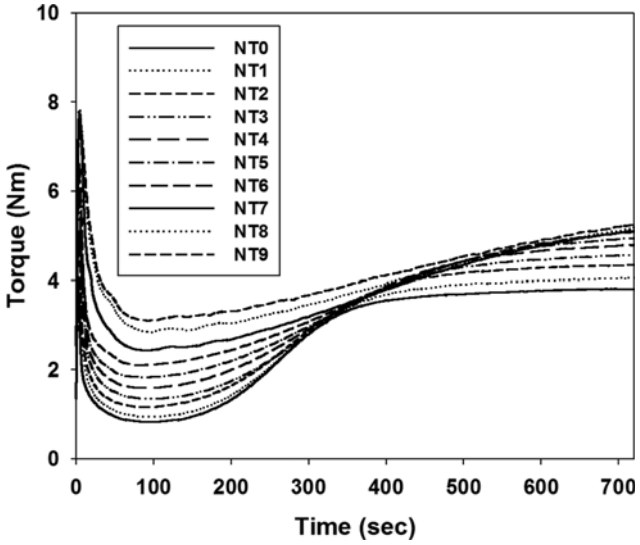

Fig. 2. Curing behavior of the MWNTs/FKM composites for various values of MWNT loading.

Fig. 2 shows the vulcanizing curves of the composites at 170 °C. The vulcanizing curve of NT0 can be divided into three stages. The first step is the induction period, which provides a safe processing time, while the second step is the curing reaction period, in which the cross-linking network forms in the rubber and the stiffness of the composite is increased. Finally, the third step is the maturing period of the cross-linking network in the composite [25]. However, distinguishing these steps from one another is difficult, and the maturing period flattens as the concentration of MWNTs is increased. It is evident that more energy is required to complete the curing process of the MWNTs-filled composites because of the decrease in the curing reaction rate at any given temperature. This may be caused by obstruction of the curing reaction due to the creation of MWNTs networks, which can restrict the movement of

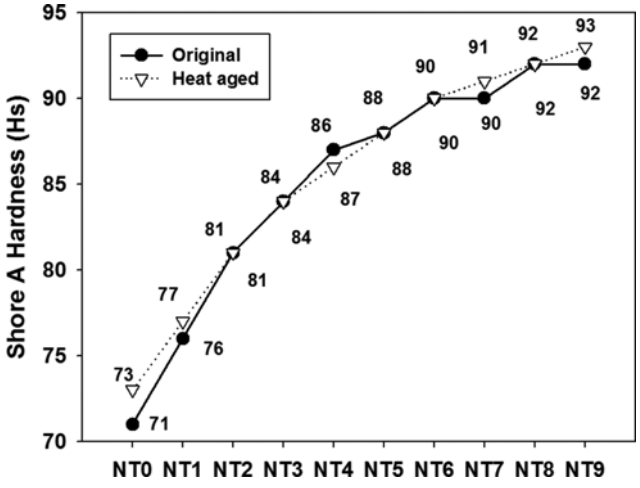

Fig. 3. Effect of MWNTs loading on hardness of FKM composites before and after heat aging.

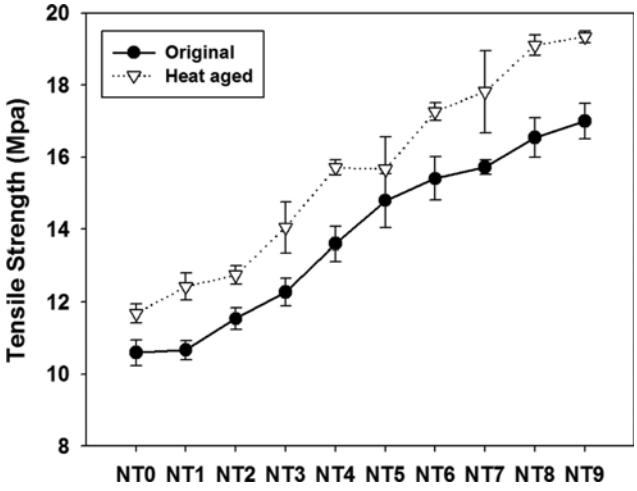

Fig. 4. Effect of MWNTs loading on tensile strength at break of FKM composites before and after heat aging.

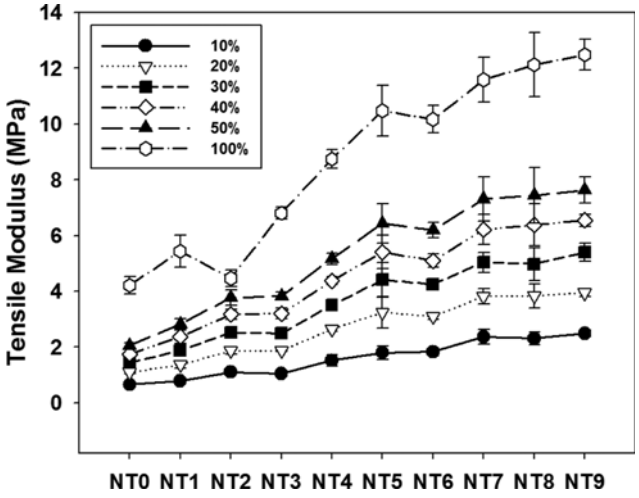

Fig. 6. Effect of MWNTs loading on tensile modulus of FKM composites for varying degrees of strain.

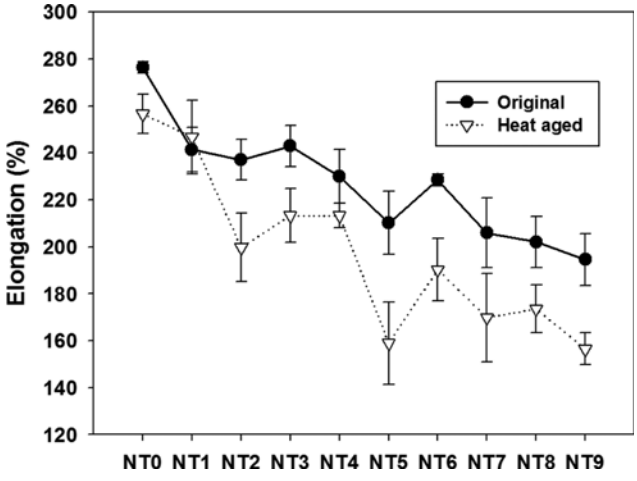

Fig. 5. Effect of MWNTs loading on elongation at break of FKM composites before and after heat aging.

rubber macromolecular chains.

2. Mechanical Properties

The Shore A hardness, tensile strength at break (T_B), and elongation at break (E_B) of the MWNTs/FKM composites before and after thermal aging are compared in Figs. 3, 4, and 5, respectively. Fig. 3 shows that the Shore A hardness increased as the amount of MWNTs was increased. A 5 Hs increase in hardness was achieved with the addition of only 1 phr of MWNTs. However, as MWNTs loading was increased in the FKM matrix, this hardness-reinforcing effect decreased gradually. Furthermore, there was a small change in hardness after thermal aging, which clearly illustrates the fact that MWNTs concentration of the composite has a considerable effect on its hardness.

The addition of MWNTs in FKM led to an increase in T_B of the composite. The T_B started to increase at 2 phr, and continued to do so with further increase in the MWNTs loading. In the case of NT 9, an increase in T_B of 6.4 MPa was achieved as compared to the unloaded specimen. One possible reason for this may be that the entangled MWNTs in contact with FKM chains in the matrix can absorb and transfer external stress during testing. On the other hand, the E_B of the composite decreased from 276% to 194% as the MWNTs concentration in FKM matrix was increased. This is due to the reduction in mobility of the FKM chains as the MWNTs loading are increased. The T_B and E_B of thermally aged specimen are also shown Fig. 4 and 5. It can be recognized that the T_B after thermal aging was higher than before thermal aging, whereas a reduction in E_B was observed for all aged specimens as compared to the unloaded specimen. This is attributed to the formation of additional cross-links, which is a well-known effect of post curing. When the degree of cross-linking after thermal aging exceeds an optimum value, the cross-linking networks become dense, which leads to an increase in tensile strength and a decrease in the mobility of the FKM chains [28].

The tensile modulus of the composites for varying degrees of strain is shown in Fig. 6. Although the cross-linking density, which could affect the modulus decreases beyond 4 phr loading as discussed previously, the modulus with strains of 10% to 100% increased gradually as the MWNTs loading was increased. This phenomenon can be explained by looking at the MWNTs morphology stated in the further section where MWNTs form a complex network, which enhanced the physical strength of the composite. From the result, it can be assumed that the MWNTs networks play a significant role in reinforcing the FKM matrix without leading to breakage of the MWNTs themselves under uniaxial deformation.

To measure the ability of the MWNTs/FKM composites to retain elastic properties after aging and under compressive stress, a compression set (CS) test was performed at 180 °C for 70 h. Compression set is a standard test for evaluating the elastic behavior of composites [29]. As shown in Fig. 7, as the amount of MWNTs was increased, the CS value increased accordingly. The CS of the composite filled with 0-7 phr MWNTs increased linearly, while composite filled with 9 phr MWNTs increased sharply. This is likely caused by a decrease in the number of chemical cross-links, which are responsible for compressive stress in the composite. Elastic recov-

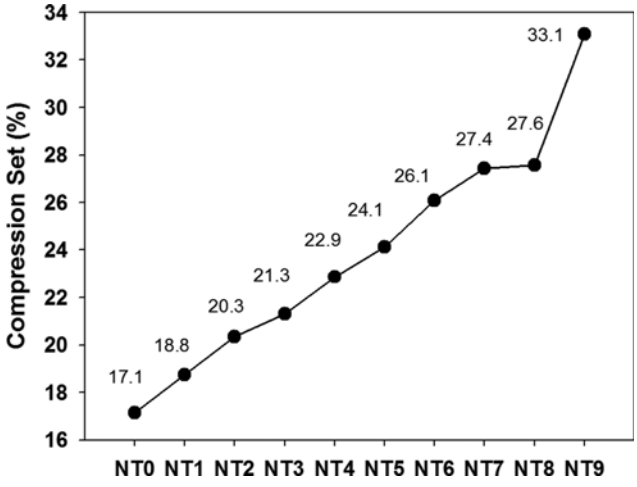

Fig. 7. Effect of MWNTs loading on compression set of FKM composites.

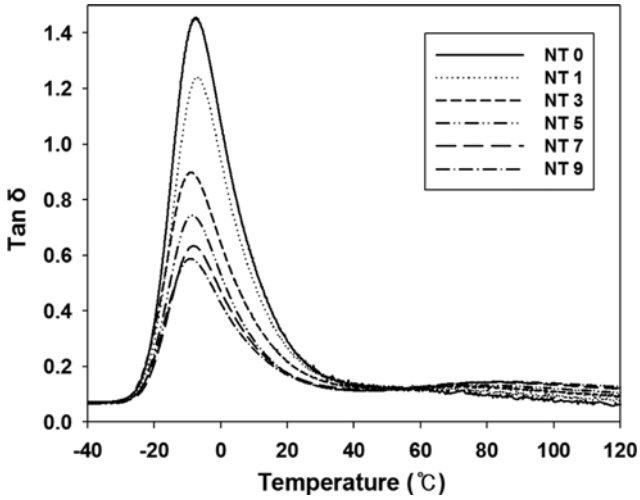

Fig. 9. Variation of tan δ of MWNTs/FKM composite as function of temperature.

ery is greater as the number of chemical cross-links increases. Another possible explanation is an increase in the number of deformable physical cross-links and a reduction in the mobility of rubber chains, which can also affect the elastic recovery. An increase in physical cross-links increases the composite's potential viscoelastic deformation [29,30]. Consequently, it is postulated that this increase in CS with the addition of MWNTs results from both the decrease in chemical cross-links and the increase in physical cross-links.

3. Dynamic Mechanical Analysis (DMA)

The storage modulus (E') represents the capability of a material to store mechanical energy and resist deformation. Fig. 8 exhibits the storage modulus of MWNTs/FKM composites. From this figure, it can be clearly observed that the storage modulus of the composites was increased with increasing MWNTs concentrations. From the significant rise in storage modulus can be explained the formation of filler networks which will be dealt in more detail in the later section.

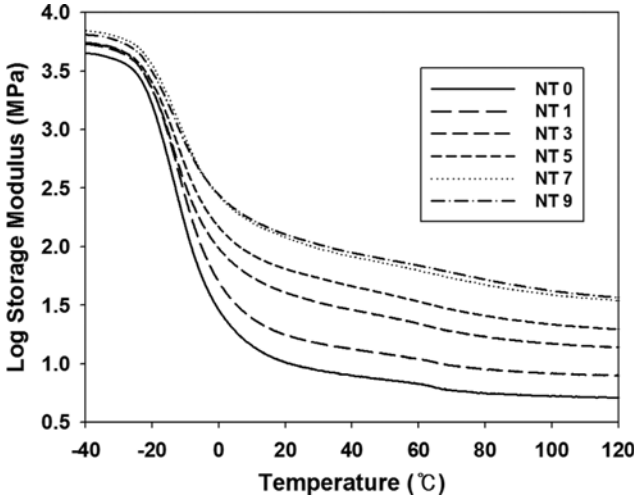

Fig. 8. Variation of storage modulus of MWNTs/FKM composites as function of temperature.

Fig. 9 exhibits the tan δ curves of MWNTs/FKM composites from a temperature sweep. From the curve at low temperature region, peak height, peak width and temperature at the peak can be compared between samples. From these values, it is possible to do a relative comparison of the polymer-filler interactions, cross-linking density, and glass transition temperature of the composites. Tan δ peak height decreased from 1.46 to 0.59 as the MWNTs concentration increased. This energy dissipation has strong correlation with the polymer-filler interactions. The polarity of FKM allows specific interactions between CNT and FKM which binds the rubber. As interactions between polymer-filler are increased, the available free-chains are decreased, resulting in a decrease in tan δ height [31,32]. Therefore, progressive decrease in tan δ as increasing the MWNTs loading can be explained by higher interaction between FKM polymer.The width of the tan δ peak can be related to the cross-linking density, and it shows a narrow curve due to the increase in MWNTs concentrations. This narrowing in peak width can be explained by considering the lower cross-linking density, which leads to an overall reduction in elastic constraints imposed by the cross-link junctions [33]. This result is consistent with the result derived in CS tests. Undeniably, T_g was influenced by the polymer chain mobility. From the mechanical properties test, it was believed that the addition of MWNTs generated filler networks which restricted polymer chain mobility and significantly increased the T_g of the composites. However, the result was different from what was expected where no significant increase in T_g was observed. The tan δ peak temperature of NT 9 even appeared to be shifted 1.44 °C lower than NT 0. This can be understood by two reasons: having a decrease in cross-linking density, and the presence of higher polymer-filler interactions. In generally, decrease in cross-linking density will decrease the T_g, while increasing the polymer-filler interactions will increase the T_g as well. Therefore, a small shift of tan δ peak can be explained that higher bound rubber attenuates increased the polymer chain mobility that is derived from less cross-linking density of the composite. From this, it can be assumed that filler-filler networks have not affected the T_g value for vulcanized com-

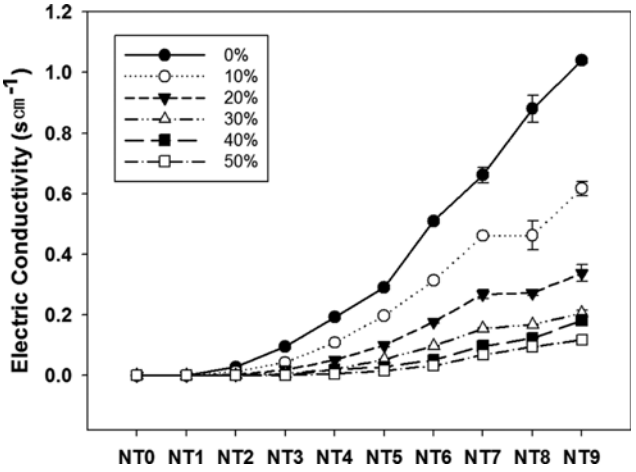

Fig. 10. Electrical conductivity of MWNTs/FKM composites as a function of MWNTs concentration.

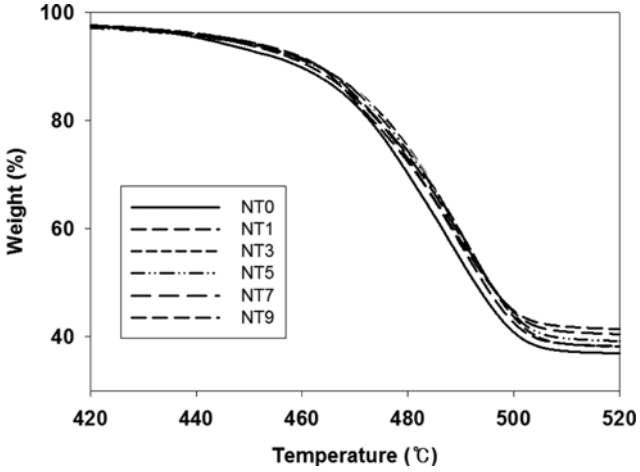

Fig. 11. TGA thermograms of MWNTs/FKM composites.

posite. Consequently, decrease in T_g for NT 9 was attributed to the fact that increased polymer chain mobility caused by less cross-linking was more dominant than decreased in polymer chain mobility by bound rubber. In rubbery state at temperature beyond 60 °C, tan δ value shows the reversed result compared to the lower temperature region. In presence of filler networks in the rubbery state, the hysteresis tended to increase slightly as the concentration of the MWNTs was increased. Increase in energy dissipation in rubber state region can be explained the slip-motion of MWNTs networks as temperature increased under cyclic deformation at low stain amplitudes.

4. Electrical Conductivity

Although rubbers are insulators, the incorporation of conductive fillers into rubber could produce a composite with reasonable electrical conductivity. As shown in Fig. 10 which demonstrates the variation of electrical conductivity of the composite with different MWNTs loading, an increase in electrical conductivity was observed from 0 to 1.039 Scm^{-1}. For the composite filled with 1 phr MWNTs without deformation, there was no enhancement in the electric conductivity. However, starting from 3 phr MWNTs an increase in the electrical conductivity was observed from 0 to 9.52×10^{-2} Scm^{-1}. This increase was caused by the formation of MWNTs networks that provided an electrical conductive pathway. The high aspect ratio of MWNTs increased the probability of filler-filler contacts, which accounts for increase in electrical conductivity at even low loading of MWNTs [34,35].

The strain dependence on the electrical conductivity of the composite was also investigated and presented in Fig. 10. The electrical conductivity decreased with uniaxial extension from 10% to 50% as compared to the original state. The electrical conductivity dropped in a similar proportion up to 7 phr MWNTs loading. Beyond 7 phr, however, it dropped even more. In the case of 50% strain for NT 9, electrical conductivity decreased to 88.7%. This clearly indicates that the existing conductive networks are experiencing breakdown by stretching, which occurred even further beyond 7 phr MWNTs loading. From the results comparing the modulus of the composite with strain, it can be concluded that the breakdown of conductive networks was not caused by the fracture of the MWNTs. This is more likely due to the alteration of MWNTs orientation by slip-motion, thereby decreasing the number of filler-filler contacts.

5. Thermal Stability

TGA was performed from room temperature to 800 °C under nitrogen atmosphere to evaluate the effect of MWNTs loading on the thermal stability of the composite. Fig. 11 shows TGA thermograms for the MWNTs/FKM composites as a function of MWNTs concentration. It was believed that the addition of MWNTs would improve the thermal stability of the FKM composite due to excellent thermal stability of MWNTs. The result indicates that the onset temperature and decomposition temperature of the MWNTs/FKM composites increased slightly by the addition of MWNTs. This means that the thermal stability of MWNTs/FKM composites has been improved with the addition of MWNTs, as evidenced by the TGA results.

6. Morphology Studies

The morphology of the MWNTs/FKM composites was evaluated by FE-SEM. The cross section of each composite was obtained by brittle fracture of the specimen in liquid nitrogen. The images on the left side of Fig. 12 show the cryogenic-fractured surface of the composites; all composites exhibit a good degree of MWNTs dispersion and distribution in the FKM matrix with the exception of a few agglomerations where small, bright dots are the indication of individual MWNTs.

To observe the continuous network of MWNTs formed in the FKM matrix, the thermally treated surface of the composite was also examined. Thermal treatment was performed at 500 °C for 3 min in air to eliminate the vulcanized FKM polymer. As shown in the right-side images of Fig. 12, MWNTs networks are sparsely interconnected at 1 phr MWNTs loading while progressively more interconnected as the MWNTs concentration was increased. It is also clear that the networks are more closely formed in the FKM matrix for higher MWNTs concentrations. In the case of NT9 composite, FKM polymer remained on the surface despite of the thermal treatment. It is assumed that the formation of a continuous network structured layer of MWNTs, which act as a thermal shield, influenced the heat stability of the composite surface.

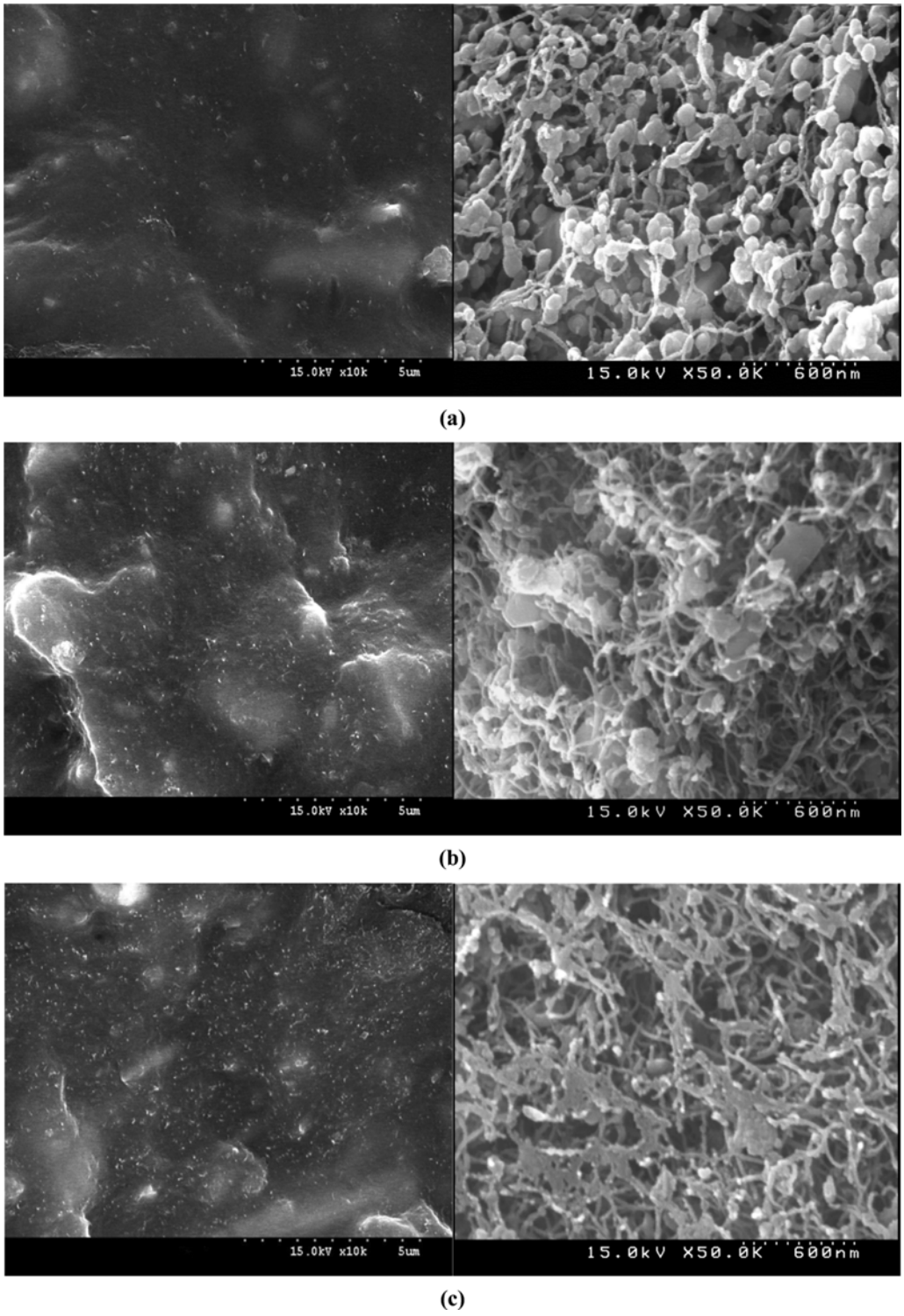

Fig. 12. SEM images of the cryogenic fractured surface (left) and thermally treated surface (right) of MWNTs/FKM composite with (a) 1 phr, (b) 3 phr, (c) 5 phr, (d) 7 phr, and (e) 9 phr.

CONCLUSIONS

We investigated the curing behavior, mechanical properties, electrical conductivity, and damping property of FKM composites with 0-9 phr MWNTs. The results indicate that the chemical cross-linking density and the curing behavior of the composites are strongly affected by MWNTs loading. This may be caused by obstruction of the curing reaction by the created MWNTs networks, which can restrict the movement of the rubber macromolecular chains. However, despite a low chemical cross-linking density of the vulcani-

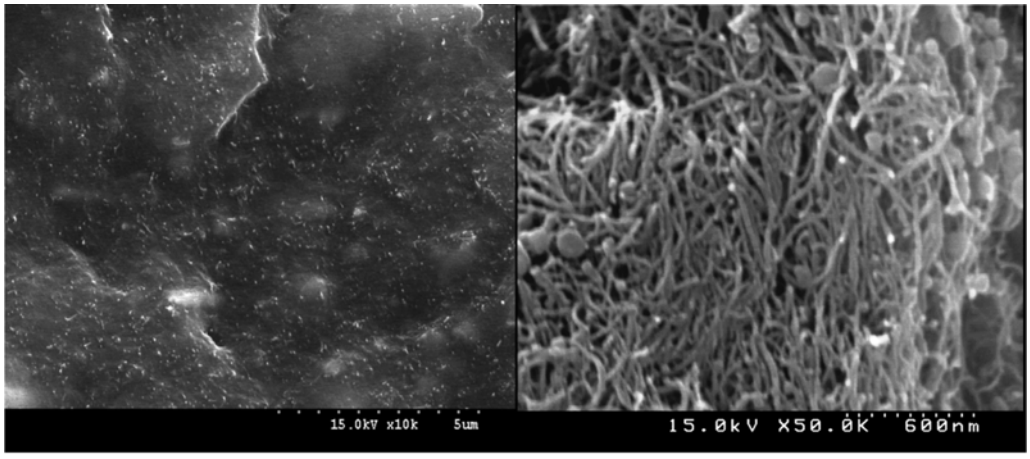

(d)

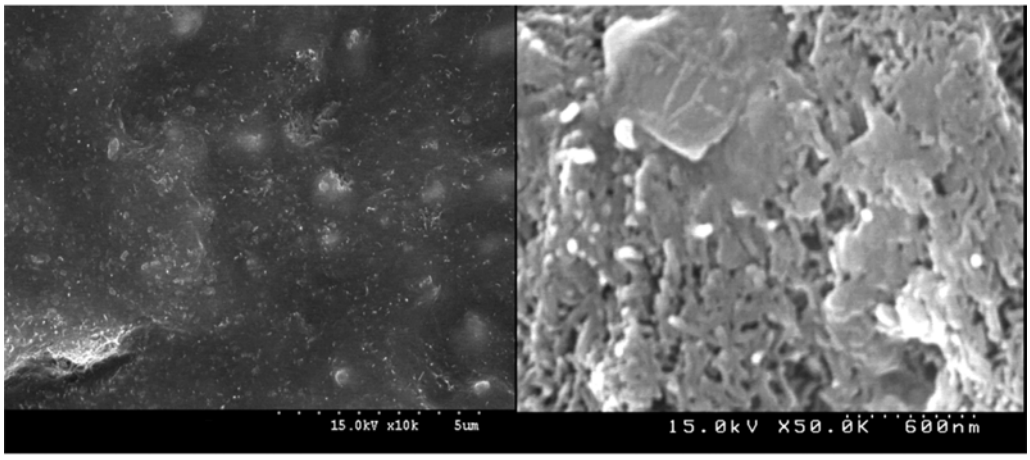

(e)

Fig. 12. Continued.

zate, the shore A hardness, tensile strength, and electrical conductivity were clearly improved. This may be due to the formation of stiff MWNTs networks, which can transfer stress and allow the flow of electrical current. Tan δ curve demonstrated improved energy dissipation at rubbery state region. TGA results indicated that the addition of MWNTs slightly increased thermal stability of FKM composite. The FE-SEM images proved not only a good degree of MWNTs dispersion and distribution in the FKM matrix, but also successfully showed that MWNT networks formed even at a low loading level due to high aspect ratio of MWNTs. From these results, it was deduced that networks of MWNTs, which possess excellent mechanical and electrical properties, strongly influenced the mechanical, electrical, and damping properties of FKM based composite. This research will therefore be useful in the development of rubber composites for fuel system components, which are deformed or vibrated while in operation.

ACKNOWLEDGEMENTS

This work was supported by the Human Resource Training Program for Regional Innovation through the Ministry of Education and National Research Foundation of Korea (NRF-2013H1B8A2032183).

REFERENCES

1. S. Akhlaghi, U. W. Gedde and M. S. Hedenqvist, *Renew. Sustainable Energy Rev.*, **43**, 1238 (2015).
2. J. Gao, Z. Gu, G. Song, P. Li and W. Liu, *Appl. Clay Sci.*, **42**, 272 (2008).
3. http://www.trelleborg.com/en/Elastomer-Laminates/Rubber-Sheeting/VITON/.
4. T. Russell, J. Walder and A. Rich, *Sealing Technol.*, **11**, 12 (2005).
5. H. Lorenz, J. Fritzsche, A. Das, K. W. Stockelhuber, R. Jurk, G. Geinrich and M. Kluppel, *Compos. Sci. Technol.*, **69**, 2135 (2009).
6. J. S. Dick, in Rubber Technology, J. S. Dick Eds., Hanser Publishers (2001).
7. J. L. White and K. Kim, Thermoplastic and Rubber Compounds, Hanser Publishers (2008).
8. L. Bokobza and O. Rapoport, *J. Appl. Polym. Sci.*, **85**, 2301 (2002).
9. L. Bokobza, *Polym. J.*, **48**, 4907 (2007).
10. M. Abdul Kader and C. Nah, *Polymer*, **45**, 2237 (2004).
11. Y. Geng, M. Y. Liu, J. Li, X. M. Shi and J. K. Kim, *Composites Part A*, **39**, 1876 (2008).
12. G. Beyer, *Fire Mater.*, **26**, 291 (2002).
13. S. Iijima, *Nature*, **354**, 56 (1991).

14. S. H. Lee, S. H. Choi, J. I. Choi, J. R. Lee and J. R. Youn, *Korean J. Chem. Eng.*, **27**(2), 658 (2010).
15. Y. S. Song, PhD thesis, Seoul National University (2004).
16. D. Tomanek, A. Jorio, M. Dresselhaus and G. Dresselhaus, in Carbon Nanotubes, A. Jorio, G. Dresselhaus and M. Dresselhaus Eds., Springer-Verlag Berlin (2008).
17. T. W. Ebbesen, H. J. Lezec, H. Hiura, J. W. Bennett, H. F. Ghaemi and T. Thio, *Nature*, **382**, 54 (1996).
18. A. D. Falco, S. Goyanes, G. H. Rubiolo, I. Mondragon and A. Marzoccz, *Appl. Surf. Sci.*, **254**, 262 (2007).
19. W. K. Park and J. H. Kim, *Macromol. Res.*, **13**, 206 (2005).
20. H. Ha, K. Ha and S. Kim, *Macromol. Res.*, **18**(5), 512 (2010).
21. H. Ha, K. Ha and S. Kim, *Macromol. Res.*, **18**(7), 660 (2010).
22. H. Ha, K. Ha and S. Kim, *Macromol. Res.*, **18**(7), 674 (2010).
23. L. Lan, Z. Yinghao, Z. Yong, O. Christopher and G. Sharon, *Appl. Surf. Sci.*, **255**, 2162 (2008).
24. Nanocyl, NC7000 Technical Datasheet. http://www.nanocyl.com/en/content/download/417/2536/file/DM-Qual-05-TDS%20NC7000-V05.pdf.
25. A. B. Sullivan and R. W. Wise, in Rubber Technology, M. Morton Eds., Kluwer Academic Publisher (1999).
26. M. Abdalla, D. Dean, P. Robinson and E. Nyairo, *Polymer*, **49**, 3310 (2008).
27. G. Sui, W. H. Zhong, X. P. Yang and Y. H. Yu, *Mater. Sci. Eng.*, A, **485**, 524 (2008).
28. N. Rattanasom and S. Prasertsri, *Polym. Test.*, **28**, 270 (2009).
29. M. Schuur and R. J. Gaymans, *Polymer*, **46**, 6862 (2005).
30. A. Mostafa, A. Abouel-Kasem, M. R. Bayoumi and M. G. El-Sebaie, *Mater. Des.*, **30**, 1561 (2009).
31. S. Mitra, K. Naskar and A. Bhowmick, in Thermal analysis of rubbers and rubbery materials, N. R. Choudhury, P. P. De and N. K. Dutta Eds., Smithers Rapra Technology (2010).
32. J. Heidarian and A. Hassan, *Composites Part B*, **58**, 166 (2014).
33. I. D. Sideridou, E. C. Vouvoudi and E. A. Adamidou, *Dent. Mater.*, **31**, 154 (2015).
34. H. Ha, K. Ha and S. Kim, *Carbon*, **48**, 1939 (2010).
35. A. Allaoui, S. Bai, H. M. Cheng and J. B. Bai, *Compos. Sci. Technol.*, **62**, 1993 (2002).